Wireless Measurement Electronics for Passive Temperature Sensor

Emilio Sardini, *Member, IEEE*, and Mauro Serpelloni, *Member, IEEE*

***Abstract*—High-temperature measurement systems do not allow the use of traditional measurement techniques. In the presence of high temperatures, the proper functioning of electronics is compromised. Furthermore, if the measurement environment is also hermetic, the traditional cabled measurement technique cannot be adopted. In this paper, a system composed by a passive sensor placed in the harsh environment and a dedicated readout electronics placed outside in a safe zone is designed and proposed for measuring the temperature up to 330 °C. The sensing element is based on a hybrid sensor constituted solely by passive components (an inductor connected to a planar micromachined variable capacitor). The hybrid sensor can be placed inside high-temperature and hermetic measuring environment, while the temperature data can be measured telemetrically by an external reading unit, located in the safe environment. In this paper, the system is presented using novel electronic circuits of the readout unit, which permit to avoid the need of an expensive commercial impedance analyzer. The wireless measurement electronics was designed and characterized; the results obtained and reported in this paper are quite in good agreement with those measured by a reference commercial impedance analyzer. The complete measurement system is presented as a viable solution to the measurement of high temperatures in harsh or enclosed industrial environments.**

***Index Terms*—Autonomous sensor, contactless telemetric system, high-temperature measurement, microelectromechanical systems (MEMS), wireless system.**

I. Introduction

IN INDUSTRIAL environments, high-temperature measurements are required for process control, safety evaluation, reliability prediction, product liability, and quality control. Since the measurement environment is harsh, it is insulated from the external side where the control or processing electronics is placed. Furthermore, in several applications such as in controlled drying processes and pressurized fluids, the environment must be hermetic as well. In these cases, the environment is commonly unsuitable for electronic active circuits since they do not work in the presence of temperatures greater than 100 °C, thus excluding the possibility of using commonly known wireless sensor network. Moreover, most existing temperature sensors cannot be used since they require a cabled solution. The solution is to measure high temperatures without contact. In contactless techniques, the sensing element is positioned in the harsh environment, while the second part of the measurement system, consisting of the active devices of the conditioning electronics required to extract the measurement information, is outside in a safe zone. In the literature, several examples of contactless measurements are reported using optical sensors [1]–[4]. Optical instruments such as pyrometers or infrared (IR) optical sensors sometimes offer a solution. In [3], an IR temperature measurement system able to measure between 500 °C and 1300 °C is described. In [4], the authors propose the use of microwave radiometry to noninvasively measure and control the temperature during the microwave sintering processes. A different measurement approach is described in [5]; the authors present a contactless magnetic measurement solution: NiFe sensors, whose properties are very sensitive to temperature, are associated to remote magnetic transducers, and the active part is placed outside. In [6], surface-acoustic-wave sensors for high-temperature applications are analyzed highlighting the material issues: The high-temperature characteristics of novel devices are investigated by finite-element simulation and by experimental deformation analysis. Assembly, interconnection, and packaging techniques are also discussed. In [7], materials and packaging solution for microsensors, systems, and devices for high-temperature and harsh environment are analyzed and compared. In [8], silicon carbide microelectromechanical systems (MEMS) are proposed for harsh environment measurements; in the paper, there is a discussion of silicon carbide MEMS as high-temperature sensors. Among the contactless systems, autonomous sensors are an interesting solution for connecting the probe positioned in the hazardous zone with the conditioning electronics in the safe zone. They represent a viable solution when the measurement environment is contained in an enclosed and hermetic space and the required wire link through the separating wall, between the harsh and safe zones, is not possible due to the presence of high pressure or to the use of expensive connecting techniques. Usually, sensing techniques are based on a change of the resonant frequency of an LC circuit. In the literature, examples of such systems are reported in [9]–[13]. In [13], a passive wireless temperature sensor operating in harsh environment for high-temperature (up to 235 °C) rotating component monitoring is reported. Contactless measurement techniques require also the use of special electronic systems. Several of these are based on frequency analysis or on impedance variation. In the literature, different proposals are reported in order to design *ad hoc* instruments for the applications. The design of electronic circuits for impedance analysis and scanning frequency can be developed in different ways,

Manuscript received April 6, 2011; revised January 2, 2012; accepted February 14, 2012. The Associate Editor coordinating the review process for this paper was Dr. Deniz Gurkan.

The authors are with the Department of Information Engineering, University of Brescia, 25123 Brescia, Italy (e-mail: mauro.serpelloni@ing.unibs.it; emilio.sardini@ing.unibs.it).

Color versions of one or more of the figures in this paper are available online at http://ieeexplore.ieee.org.

Digital Object Identifier 10.1109/TIM.2012.2199189

with a field-programmable-gate-array approach [14], [15] or with an impedance analyzer [16], [17]. In [17], the impedance measurement instrumentation is based on the measurement of the real and the imaginary part of impedance, working in the frequency from 10 to 100 kHz. In [18], the authors describe an impedance gain-phase analyzer; the instrument operates in the frequency range of 10 Hz–200 kHz.

In this paper, the authors propose a complete wireless measurement system of temperature up to 330 °C inside high-temperature and/or hermetic environment. Two papers previously published describe the adopted hybrid sensor. In [19] and [20], a novel temperature sensor composed by a hybrid MEMS is described and characterized. The sensor measures high temperatures in harsh industrial environments. The hybrid MEMS is composed by a planar inductor developed in thick-film technology and a micromachined variable capacitor that is temperature sensitive [21]. In [19] and [20], an expensive commercial impedance amplifier was used to measure the module and phase of the impedance at the terminals of a readout inductor placed in a safe zone. In [22], a novel high-temperature measurement system composed by the hybrid MEMS as the temperature sensor and a contactless front-end electronic is briefly described. The electronic circuits implement a telemetric technique, avoiding the need of an expensive commercial impedance amplifier. In this paper, the proposed wireless measurement system is widely described; important aspects about how it has been designed, implemented, and tested are reported. Particular attention is given to the aspects of design and testing of the developed electronic circuits. The electronics is based on a measurement technique called three-resonance method [19]. The distance between the sensor and reader can be constant if the telemetric system is fixed with the measuring chamber; otherwise, the measurement system consists of the sensor placed in the oven and a mobile unit outside. The proposed system is capable of operating in both situations. To experimentally verify the characteristics of the proposed measurement system, a temperature-controlled measurement oven has been developed. In this paper, a comparison between the developed circuits and a commercial impedance analyzer is performed. The analysis shows that the proposed circuits allow the measurement of the frequencies in a satisfactory manner, permitting a good telemetric measurement of the temperature up to 330 °C.

II. Description of the Temperature Measurement System

The proposed telemetric system is shown schematically in Fig. 1: On the left, the hybrid MEMS is placed into the harsh environment, while on the right, the readout unit is in the safe zone. A wall separates the two zones, and the two subsystems communicate through an inductive coupling. This wall must be composed of nonmagnetic and nonconductive material so that the magnetic coupling is guaranteed.

A. Hybrid MEMS

The hybrid MEMS placed in the harsh environment is composed by a microfabricated temperature-sensitive variable

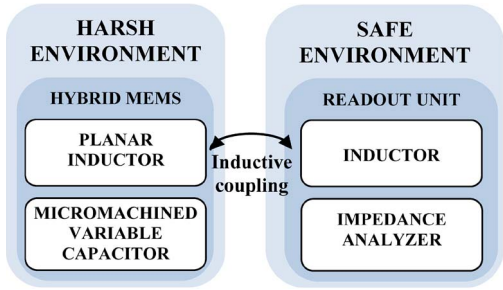

Fig. 1. Block diagram of the telemetric system.

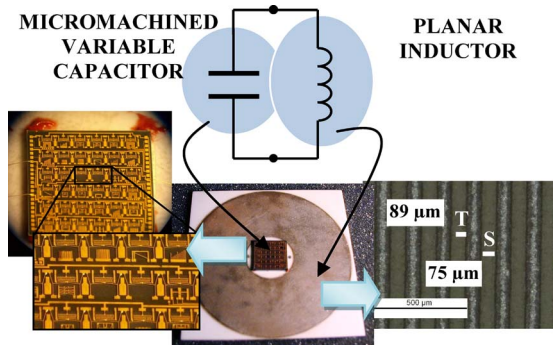

Fig. 2. Pictures of the hybrid MEMS.

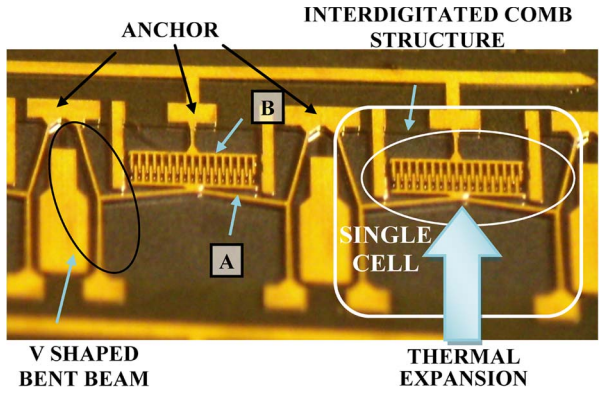

Fig. 3. Microscope picture of the bent beam.

capacitor fabricated using the MetalMUMPs process [21] and a planar inductor with high-temperature characteristics developed in thick-film process (see Fig. 2). The hybrid MEMS behaves as an LC resonant circuit, where the capacitance is the micromachined variable capacitor and the inductance is the planar inductor. The layout of the variable capacitor is organized in 36 cells having capacitive behavior and connected in parallel. The interdigitated capacitor is made by two structures named A and B in Fig. 3. The thermal expansion generates a relative movement of the A-structure and the B-structure, varying the capacitance. The maximum operating temperature is limited by the maximum operating limit of nickel (350 °C). The single cell (see Fig. 3) is based on a cascade of three bent beam structures. The planar inductor is obtained using thick-film technology by screen printing and microcutting by a laser. During the screen printing, two conductive (QM14 commercialized by DuPont) films, one overlapping the other, were deposited to reach a thickness of

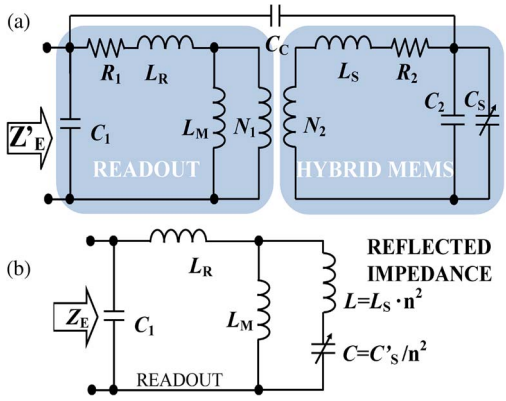

Fig. 4. (a) Telemetric inductive model. (b) Simplified model.

about 20 μm over an alumina substrate (50 mm $\times$ 50 mm $\times$ 0.63 mm). The conductive film has a resistivity of about 1.5–2.5 mΩ/sq. The deposited film was dried for 10–15 min at 150 °C and then was fired in a conveyor furnace for 30 min with a peak temperature of 850 °C. The microcutting process consists of material ablation by a laser. The inductors have the external diameter of 50 mm, 120 windings each of about 89-μm width and spaced 75 μm from the others. The die is fixed to the planar inductor by a high-temperature ceramic adhesive (Resbond 931C) commercialized by Cotronics. The contact pads are bonded to the inductor terminals. The mass of the hybrid MEMS is about 8 g: 6 g (alumina) and 0.2 g (die), and the remaining mass is due to the glue. The hybrid MEMS characterization is reported in [20], and two consecutive processes of heating and cooling have been monitored using the hybrid sensor connected to an impedance analyzer (HP4194A); a good repeatability and no relevant hysteretic phenomena have been observed.

B. Telemetric Model

An inductor, labeled readout inductor, is placed close to the hybrid MEMS but outside in the safe environment: The two inductors constitute the telemetric coupled system. The readout inductor is directly connected to the conditioning electronics. The readout inductor is a planar spiral fabricated in thick-film technology, and it has 30 windings, each of 250-μm width and spaced 250 μm from the others. The external diameter is 50 mm wide. The readout inductor and the hybrid MEMS were modeled as reported in Fig. 4. R_1, R_2 are the equivalent resistances of the readout and sensor. C_1, C_2 are the parasitic capacitances of the readout inductor and planar inductor, while C_S is the capacitance of the variable capacitor. L_R, L_S are the readout and sensor leakage inductances. L_M is referred to as the coupled flux. N_1 and N_2 are the equivalent numbers of the inductor windings, and C_C is the coupling capacitance. Due to the geometry of the system, the coupling capacitance C_C can be neglected. Whereas the working frequency range is high, the resistances R_1, R_2 can be neglected since they have impedances of much less value than those of the series inductor L_R, L_S. L and C are L_S and C'_S as seen from the primary of the ideal transformer, and parameter "n" is the ratio between N_1 and N_2. C'_S is the parallel of C_2 and C_S.

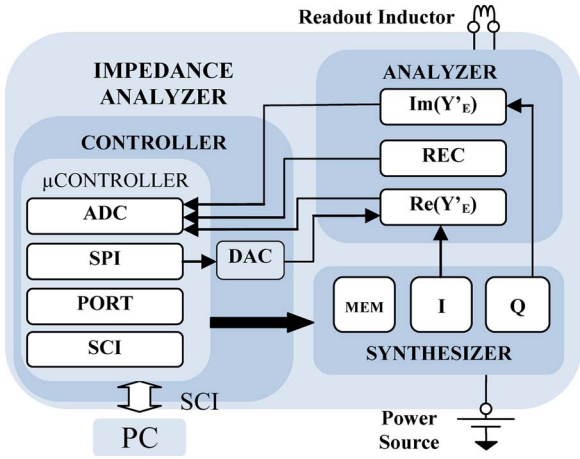

Fig. 5. Block diagram of the conditioning electronics.

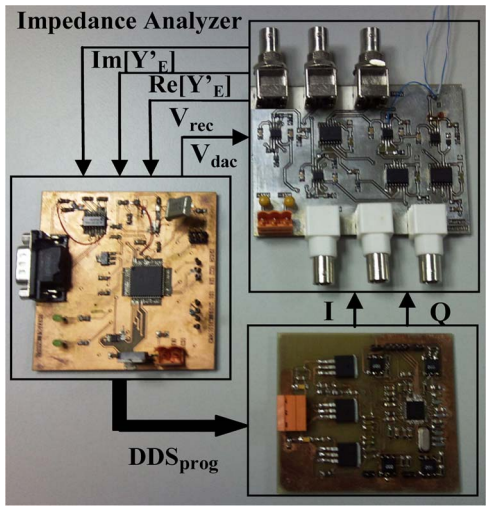

Fig. 6. Photograph of the electronic circuits realized in printed circuit board technology.

C. Conditioning Electronics

In this section, the proposed conditioning electronics for impedance measurement is presented. The impedance analyzer is composed of a synthesizer for the generation of the reference signals, an analyzer of the real and the imaginary part of the admittance, and a controller composed of a microcontroller and a digital–analog converter (DAC). A schematic of the proposed circuit is shown in Fig. 5, and a photograph of the electronic circuit is shown in Fig. 6.

1) Synthesizer: The synthesizer consists of a direct digital synthesizer, commercialized by Analog Devices (AD9959); it can generate waveforms with an internal clock speed of 500 mega-samples per second, a frequency tuning accuracy of 32 b, and a phase tuning accuracy of 14 b. This device generates two signals. The first one is the in-phase signal (labeled as I in Fig. 5), and it is used to drive the telemetric system and to extract the real part of Y'_E admittance. The second signal is the quadrature signal, (labeled as Q in Fig. 5) used for extracting the imaginary part of Y'_E.

2) Analyzer: The block diagram of the analyzer is shown in Fig. 7. The system contains three analog multipliers

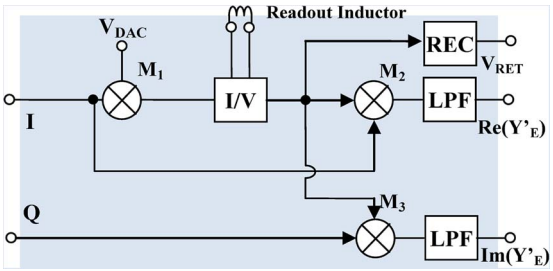

Fig. 7. Block diagram of the analyzer.

(Intersil HA2556), each of four-quadrant type, and two passive low-pass filters. The function of the circuit is to extract the real and imaginary admittance components and identify the resonant frequencies for the measuring technique. A sinusoidal voltage, whose amplitude and frequency are respectively regulated by V_{DAC} and I, is applied to the telemetric system. The injected current is successively sent to the M_2 multiplier since the other input of the multiplier is again the in-phase signal (I). The output of the low-pass filter is the real component of the voltage that is successively acquired by an analog–digital converter (ADC) and further processed by a microcontroller. Similarly, also the imaginary component has been obtained by multiplying the voltage of the telemetric system with the Q signal. After the multiplication and the low-pass filter, the imaginary component is sampled by the ADC converter.

3) Controller: The controller is composed by a microcontroller, commercialized by Freescale (MCF51AC256), and a DAC. The microcontroller integrates the Serial Peripheral Interface and Serial Communication Interface (SCI) and at least three channels of 10-b ADC. The sampling time of the ADC can be adjusted by programming the microcontroller's specific registries. Since the signal from the three channels is a continuous signal and the lower limit of the frequency of interest is 1 MHz and considering that the change in temperature is a slow process, the sampling time was not considered a restrictive parameter for the process. For the performed measurements, this time is 2 ms for each frequency set, but this value can certainly be lowered. The ADC samples the real $(\mathrm{Re}(Y'_E))$, imaginary $(\mathrm{Im}(Y'_E))$, and peak RECtifier (REC) of the telemetric voltage. The REC signal is the output of a full bridge diode Schottky and is used by the microcontroller to regulate the amplitude of the injecting current into the telemetric system. The aim is to avoid the saturation of the multiplier since the impedance module of the telemetric system has a wide dynamic. The microcontroller programs the synthesizer in order to sweep the frequency from 1 to 10 MHz, and during this phase, the microcontroller stores the sampled data into its internal memory and, when the sweep has finished, starts the data processing. The number of samples acquired during measurement is a number settable by user. After this process, the microcontroller sends the data to a personal computer (PC) through the SCI,

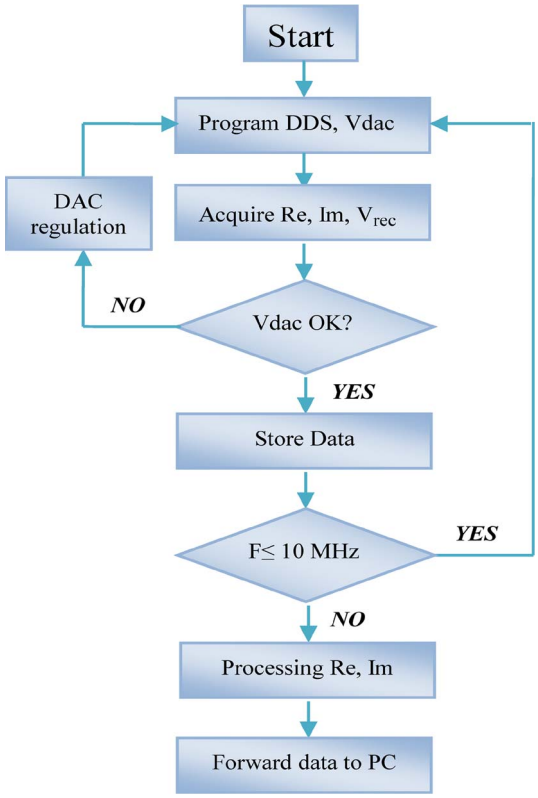

Fig. 8. Flowchart of measurement system.

and the PC analyzes the module and the phase of impedance extracting the frequencies of interest required by the three-resonance method. In Fig. 8, the flow chart of the measurement system is represented. As it can be seen from the diagram, the value of V_{rec} is constantly monitored. The regulation by DAC is then carried out automatically only when needed.

III. Measurement Technique

Referring to the circuit shown in Fig. 4, Z_E is calculated as (1) shown at the bottom of the page.

The impedance reported in (1) has three resonant frequencies. The first (f_{ra}) and the second resonant frequency (f_{rb}) are both influenced by C_1 and C. The resonant frequency (f_a) is influenced only by C, and it is more sensitive to C than the other two frequencies. Its expression is

$$f_a = \frac{1}{2\pi\sqrt{C \cdot \left(L + \frac{L_M L_R}{L_R + L_M}\right)}}. \tag{2}$$

f_a depends on C and also on distance since the distance changes the coupled and the leakage flux modifying the value of L_M, L_R. The other two frequencies (f_{ra} and f_{rb}) have more complex dependence and are dependent also on the parasitic

$$Z_E = \frac{s^3\left(L_M LC + L_R C(L_M + L)\right) + s(L_M + L_R)}{s^4 C_1\left(L_M LC + L_R C(L_M + L)\right) + s^2\left(C_1(L_M + L_R) + C(L_M + L)\right) + 1} \tag{1}$$

capacitance of the readout inductor. If the two elements of the telemetric system are fixed between the walls of the oven, the distance does not change, and the sensor capacitance can be obtained from (2). Anyway, if the conditioning electronics is mounted over a mobile unit or the distance between the readout and hybrid sensor changes for any reason, the changing of the distance is compensated by the three-resonance method [19]. This method is based on a parameter, called "F," whose value depends only on distance

$$F = (2\pi f_{r_a})^2 + (2\pi f_{r_b})^2 - (2\pi f_a)^2 = \frac{1}{C_1\left(L_R + \frac{L_M L}{L_M + L}\right)}. \tag{3}$$

If C_1 is fixed, "F" depends only on coupled and leakage fluxes: These values are related only to the distance and not to the transducer capacitance. Moreover, the parameter "F" is obtained by a direct measurement since it can be calculated by elaborating the measurement of the three f_{ra}, f_{rb}, and f_a frequencies. Introducing the following expressions:

$$L = L_S \cdot n^2 \tag{4}$$

$$C = \frac{C'_S}{n^2} \tag{5}$$

$$L_1 = L_R + L_M \tag{6}$$

$$L_2 = L_S + \frac{L_M}{n^2}. \tag{7}$$

Substituting (4)–(7) into (2) and in (3) and rearranging the expressions, the ratio of (3) with (2) is equal to

$$\frac{F}{(2\pi f_a)^2} = \frac{L_2 C'_S}{L_1 C_1}. \tag{8}$$

Rearranging (8), a straightforward expression of the sensor capacitance (C'_S) is

$$C'_S = \frac{L_1 C_1}{L_2} \frac{F}{(2\pi f_a)^2}. \tag{9}$$

C'_S is obtained as a product between a constant term and a second one calculated from the three measured f_{ra}, f_{rb}, and f_a frequencies. The constant term can be automatically obtained from a calibration operation or can be calculated measuring the equivalent circuit parameters of each single planar inductor: L_1 and L_2 are the self-inductances of the readout and sensing inductances, while C_1 is the parasitic capacitance (or any other added capacitance) of the readout circuit. The equivalent circuit parameters of every single inductor separately (consisting in the series of an inductance and a resistance both in parallel with a capacitance) have been measured by the impedance analyzer HP4194A, and their values are reported in Table I.

IV. Measurement Electronic

As previously reported, to calculate $C's$, the measurement of the three resonant frequencies (f_{ra}, f_{rb}, f_a) is required. These are the resonance frequencies of Z_E and are frequency points whose phase is zero. The impedance measured to the readout terminals is Z'_E. Its diagram is reported in Fig. 9, where it is possible to individuate three points $f'_{ra}, f'_a f'_{rb}$ that correspond in succession from right to left to the first maximum and minimum, respectively, while f'_{rb} is the second maximum. When the resistance components of the model (see Fig. 2) have zero value, the three resonant frequencies $f_{ra}, f_a f_{rb}$ and $f'_{ra}, f'_a f'_{rb}$ respectively coincide. In the real case, the resistances of the readout inductor and of the hybrid sensor have about 22 and 80 Ω at 25 °C, respectively. Their values are also subjected to change with temperature. In this case, f'_{ra}, f'_a does not coincide with f_{ra}, f_a. The error introduced in the calculation of C'_S using f'_{ra}, f'_a instead of f_{ra}, f_a has been estimated, and it is reported in Fig. 10 as a function of the resistance values. The data have been obtained from Spice simulation. Physical models of the readout inductor and hybrid sensor have been tuned up from experimental measurement. The simulation results are shown in Fig. 10, where the values of f'_{ra}, f'_a are reported as a function of the resistance. The values of f_{ra}, f_a are 1.125 and 1.179 MHz.

Approximately, the resistance values of the model representing the real system are 80 and 22 Ω, and considering the worst

TABLE I
Equivalent Circuit Parameters

Inductors	*Inductance (μH)*	*Capacitance (pF)*	*Resistance (Ω)*
Sensing Inductor	235	1.8	80
Readout Inductor	14.5	91.4	22

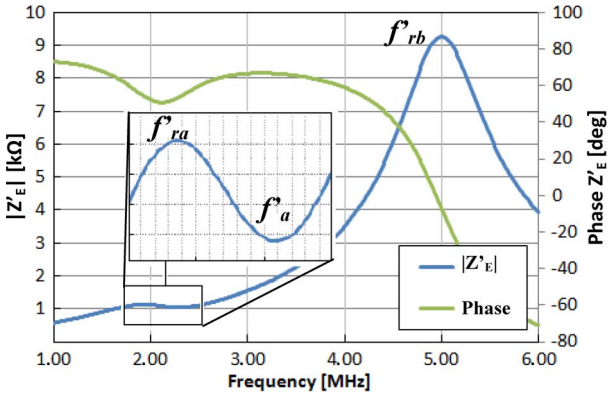

Fig. 9. Module and phase of the Z'_E impedance.

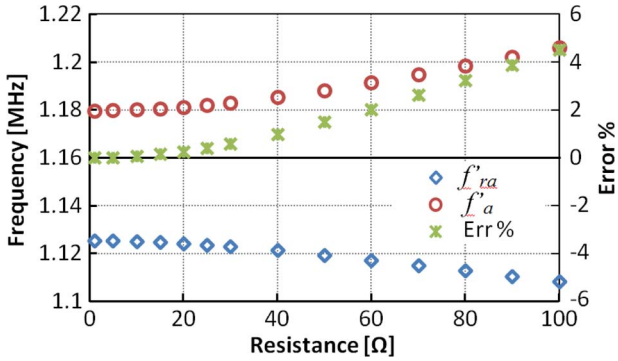

Fig. 10. Frequency f'_{ra}, f'_a values and the error in the calculation of C'_s as a function of the resistance.

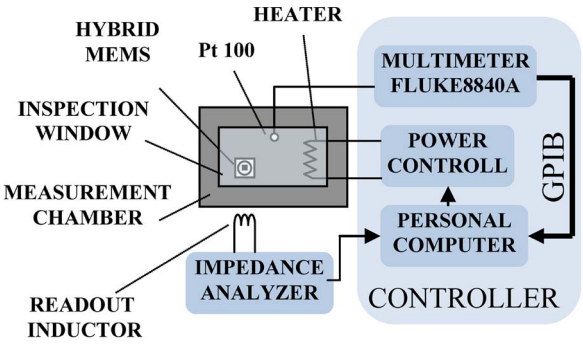

Fig. 11. Experimental setup for high-temperature measurements.

case, the error is about 3%. The measurement electronics calculates f'_{ra}, f'_{rb}, f'_a values acquiring the direct value of the real and imaginary components of the admittance in a defined frequency range. Subsequently, the modulus and phase of the impedance are mathematically calculated with classical formula, and the values of the three resonant frequencies are identified: f'_{ra}, f'_a are the first maximum and minimum, respectively, while f'_{rb} is the second maximum. The output sampled signals ($\mathrm{Re}[Y'_E]$ and $\mathrm{Im}[Y'_E]$) of the electronic circuit (see Fig. 5) are proportional to the admittance of the load, and they can be represented as

$$Y'_E = A + JB. \tag{10}$$

where A is $\mathrm{Re}[Y'_E]$ and B is $\mathrm{Im}[Y'_E]$. The microcontroller implements the following equation to extract the module and phase of admittance:

$$|Y'_E| = \sqrt{\mathrm{Re}\,[Y'_E]^2 + \mathrm{Im}\,[Y'_E]^2} \tag{11}$$

$$Phase\,[Y'_E] = \arctan \frac{\mathrm{Im}\,[Y'_E]}{\mathrm{Re}\,[Y'_E]}. \tag{12}$$

After this conversion, the module and phase of impedance can be extracted

$$|Z'_E| = \frac{1}{|Y'_E|} \tag{13}$$

$$Phase\,[Z'_E] = -\,Phase\,[Y'_E]\,. \tag{14}$$

V. Experimental Setup

An experimental setup has been designed to test the measurement system at high temperatures. In Fig. 11, a block diagram of the experimental setup is shown. The measurement chamber is isolated from the outside by two walls, one of aluminum and the other of steel; between them, thermoresistive wool (Superwool607 commercialized by Thermal Ceramics) is interposed. The total thickness of the measurement chamber is about 3 cm, and the maximum space of the chamber is 30 cm × 30 cm × 13 cm. In one side, there is a window of temperate glass, whose dimensions are 12 × 12 cm, for visual inspection of the internal process. The maximum working temperature is about 500 °C. Inside the chamber, an IR heater of 500 W controls the temperature. In order to assure that internal temperature is distributed uniformly, three thermoresistances (Pt100) have been positioned in different points; each one is connected to a multimeter (Fluke 8840A). During the execution of the test, the maximum differences between the three thermoresistances have been about 0.2 Ω that corresponds to less than 1 °C. A PC, running a developed LabVIEW virtual instrument, is connected to the multimeters through an IEEE 488 bus and to the input of the power control through the digital output of the I/O board. The PC monitors the temperature inside the oven and controls the IR heater by turning on and off the power circuit. The hybrid sensor has been put inside the oven, while the readout inductor is placed outside at a distance of 10 mm from the sensor.

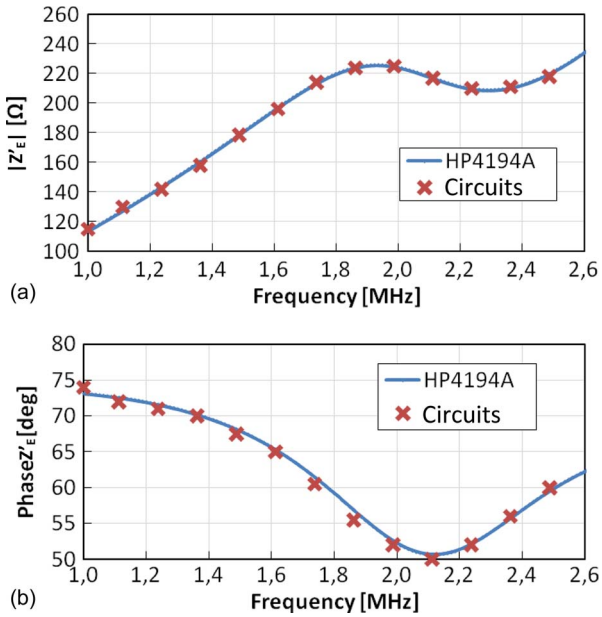

Fig. 12. (a) Module and (b) phase of the hybrid MEMS for a temperature of about 54 °C measured by HP4194A and the proposed circuits.

VI. Experimental Results

To test the telemetric measurement system, the temperature inside the oven has been changed from about 50 °C to 330 °C with steps of 20 °C. For each temperature value, the method uses three specific resonant frequencies (f_{ra}, f_{rb}, f_a) to calculate the capacitance of the sensor, and then, the flexibility of the proposed measurement system allows restricting the range of measures near the frequencies of interest to better identify the three required resonant frequencies.

Fig. 12 shows the experimental results obtained by the commercial impedance analyzer (HP4194A) and through the proposed circuits at a temperature of 54 °C. The uncertainty for the measurements obtained with the impedance analyzer is about ±700 Hz with a confidence level of 68.26%, and the uncertainty for the measurements obtained with the proposed conditioning electronics is about ±1000 Hz with a confidence level of 68.26%.

Figs. 13 and 14 show five profiles obtained interpolating the experimental data of the module and phase of the Z'_E impedance, respectively, in which two resonant frequencies (f'_{ra} and f'_a) are visible.

From previous data shown in Figs. 13 and 14, the resonance frequencies have been identified as maximum and minimum

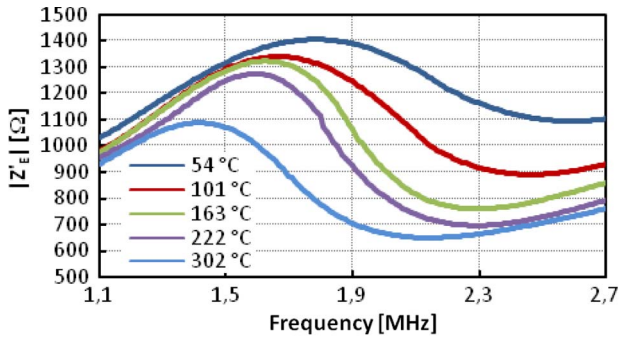

Fig. 13. Modulus of the hybrid MEMS measured with the impedance analyzer at different temperatures.

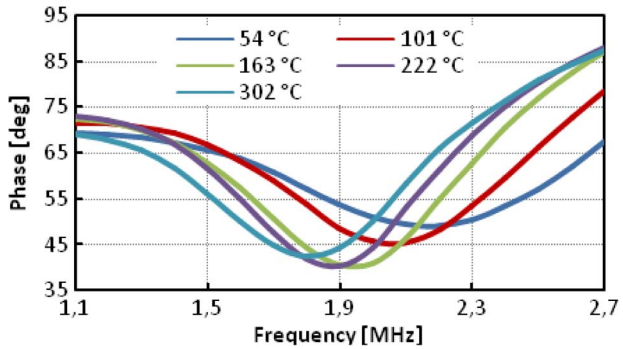

Fig. 14. Phases of the hybrid MEMS measured with the impedance analyzer at different temperatures.

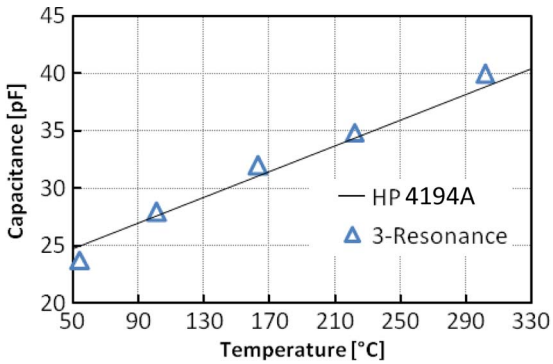

Fig. 15. Temperature compared with the impedance analyzer (HP4194A) measured capacitance and three-resonance capacitance calculated values.

points applying the three-resonance method; the values of the hybrid sensor capacitance has been calculated [see (9)]. The constant term has been obtained by a calibration operation. Results are reported in Fig. 15. In the graph (see Fig. 15), the calculated capacitances are reported and are compared with the curve obtained from a direct measurement of the hybrid sensor capacitances using an impedance analyzer (HP4194A). The experimental data fit well the capacitance values obtained by a direct measurement. The measurement results made it possible to calculate the deviation of about 1 pF between the calculated one by the proposed circuits and by the HP4194A.

VII. Conclusion

This work describes a system for measuring high temperatures in harsh environments. The system consists of a sensor placed in the measuring chamber and an external reading unit placed outside the measuring chamber in a "safe place." The sensor consists of a capacitive temperature transducer and a thick-film inductor and measures temperature up to 330 °C. The reading unit can be fixed or mobile and can operate up to distances of few centimeters. The change of distance of the readout unit can be compensated by the measurement technique used. The system was tested in the laboratory, showing good agreement with reference data.

Acknowledgment

The authors would like to thank the staff guided by Prof. Baglio of the University of Catania for the support and the technical design of the microelectromechanical systems.

References

[1] M. V. P. Kruger, M. H. Guddal, R. Belikov, A. Bhatnagar, O. Solgaard, C. Spanos, and K. Poolla, "Low power wireless readout of autonomous sensor wafer using MEMS grating light modulator," in *Proc. IEEE/LEOS Int. Conf. Optical MEMS*, 2000, pp. 67–68.

[2] S. F. Lord, S. L. Firebaugh, and A. N. Smith, "Remote measurement of temperature in the presence of a strong magnetic field," *IEEE Trans. Instrum. Meas.*, vol. 58, no. 3, pp. 674–680, Mar. 2009.

[3] J. Rodriguez, J. Meca, J. A. Jimenez, and E. J. Bueno, "Monitoring and quality improvement of pharmaceutical glass container's manufacturing process," *IEEE Trans. Instrum. Meas.*, vol. 57, no. 3, pp. 584–590, Mar. 2008.

[4] C. Beaucamp-Ricard, L. Dubois, S. Vaucher, P. Y. Cresson, T. Lasri, and J. Pribetich, "Temperature measurement by microwave radiometry: Application to microwave sintering," *IEEE Trans. Instrum. Meas.*, vol. 58, no. 5, pp. 1712–1719, May 2009.

[5] D. Mavrudieva, J. Y. Voyant, A. Kedous-Lebouc, and J. P. Yonnet, "Magnetic structures for contactless temperature sensor," *Sens. Actuators A, Phys.*, vol. 142, no. 2, pp. 464–467, Apr. 2008.

[6] J. W. Mrosk, L. Berger, C. Ettl, H. J. Fecht, G. Fischerauer, and A. Dommann, "Materials issues of SAW sensors for high-temperature applications," *IEEE Trans. Ind. Electron.*, vol. 48, no. 2, pp. 258–264, Apr. 2001.

[7] M. R. Werner and W. R. Fahrner, "Review on materials, microsensors, systems, and devices for high-temperature and harsh-environment applications," *IEEE Trans. Ind. Electron.*, vol. 48, no. 2, pp. 249–257, Apr. 2001.

[8] M. Mehregany, C. A. Zorman, N. Rajan, and W. C. Hung, "Silicon carbide MEMS for harsh environments," *Proc. IEEE*, vol. 86, no. 8, pp. 1594–1609, Aug. 1998.

[9] M. A. Fonseca, M. G. Allen, J. Kroh, and J. White, "Flexible wireless passive pressure sensors for biomedical applications," in *Proc. Tech. Dig. Solid State Sens., Actuator, Microsyst. Workshop*, Hilton Head Island, SC, Jun. 2006, pp. 37–42.

[10] Y. Jia, K. Sun, F. J. Agosto, and M. T. Quinones, "Design and characterization of a passive wireless strain sensor," *Meas. Sci. Technol.*, vol. 17, no. 11, pp. 2869–2876, Nov. 2006.

[11] E. Birdsell and M. G. Allen, "Wireless chemical sensors for high temperature environments," in *Proc. Tech. Dig. Solid-State Sens., Actuator, Microsyst. Workshop*, Hilton Head Island, SC, Jun. 2006, pp. 212–215.

[12] E. L. Tan, W. N. Ng, R. Shao, B. D. Pereles, and K. G. Ong, "A wireless, passive sensor for quantifying packaged food quality," *Sensors*, vol. 7, no. 9, pp. 1747–1756, Sep. 2007.

[13] Y. Wang, Y. Jia, Q. Chen, and Y. Wang, "A passive wireless temperature sensor for harsh environment applications," *Sensors*, vol. 8, no. 12, pp. 7982–7995, Dec. 2008.

[14] L. A. Barragan, D. Navarro, J. Acero, I. Urriza, and J. M. Burdío, "FPGA implementation of a switching frequency modulation circuit for EMI reduction in resonant inverters for induction heating appliances," *IEEE Trans. Ind. Electron.*, vol. 55, no. 1, pp. 11–20, Jan. 2008.

[15] J. Qin, C. E. Stroud, and F. F. Dai, "FPGA-based analog functional measurements for adaptive control in mixed-signal systems," *IEEE Trans. Ind. Electron.*, vol. 54, no. 4, pp. 1885–1897, Aug. 2007.

[16] A. O. Niedermayer, T. Voglhuber-Brunnmaier, E. K. Reichel, and B. Jakoby, "Improving the precision of a compact subsampling impedance

analyzer for resonating sensors," *Procedia Chem.—Proc. Eurosensors XXIII Conference*, vol. 1, no. 1, pp. 1335–1338, Sep. 2009.
[17] J. S. Riquelme, F. S. Quijano, A. Baldi, and M. T. Oses, "Low power impedance measurement integrated circuit for sensor applications," *Microelectron. J.*, vol. 40, no. 1, pp. 177–184, Jan. 2009.
[18] J. Castelló, R. García-Gil, and J. M. Espí, "A PC-based low cost impedance and gain-phase analyzer," *Measurement*, vol. 41, no. 6, pp. 631–636, Jul. 2008.
[19] D. Marioli, E. Sardini, M. Serpelloni, B. Andò, S. Baglio, N. Savalli, and C. Trigona, "Hybrid telemetric MEMS for high temperature measurements into harsh industrial environments," in *Proc. I2MTC*, Singapore, 2009, pp. 1423–1428.
[20] D. Marioli, E. Sardini, and M. Serpelloni, "Passive hybrid MEMS for high temperature telemetric measurements," *IEEE Trans. Instrum. Meas.*, vol. 59, no. 5, pp. 1353–1361, May 2010.
[21] B. Andò, S. Baglio, N. Pitrone, N. Savalli, and C. Trigona, "Bent beam MEMS temperature sensors for contactless measurements in harsh environments," in *Proc. IEEE I2MTC*, Victoria, BC, Canada, 2008, pp. 1930–1934.
[22] E. Sardini and M. Serpelloni, "High-temperature measurement system with wireless electronics for harsh environments," in *Proc. IEEE SAS*, San Antonio, TX, 2011, pp. 256–261.

Emilio Sardini (M'99) was born in Commessaggio, Mantova, Italy, in 1958. He received the Laurea degree in electronic engineering from the Politecnico di Milano, Milan, Italy, in 1983.

Since 1984, he has conducted research and teaching activities at the Department of Electronics for Automation, University of Brescia, Brescia, Italy. Since 2006, he has been a Full Professor of Electrical and Electronic Measurement with the University of Brescia. He has been a member of the Integrated Academic Senate and of the Board of Directors of the University of Brescia. For several years, he participated in the teaching organization of its faculty. He is the Coordinator of the "technology for health" Ph.D. and a member of the College of Mechatronics Ph.D. at the University of Bergamo, Bergamo, Italy. He is also the Deputy Dean of the faculty. Recently, his research has been addressed to the development of autonomous sensors. They can be passive sensors and interrogated with telemetry techniques for applications in secure environments such as inside the human body. Autonomous sensors can be equipped with conditioning electronics exploiting energy from the measurement environment. He is the author or coauthor of more than 100 papers published on international journals or proceedings of international conferences.

Mauro Serpelloni (M'12) was born in Brescia, Italy, in 1979. He received the Laurea degree (*summa cum laude*) in industrial management engineering and the Research Doctorate degree in electronic instrumentation from the University of Brescia, Brescia, in 2003 and 2007, respectively.

He is currently an Assistant Professor of electrical and electronic measurements with the Department of Information Engineering, Faculty of Engineering, University of Brescia. He has worked on several projects relating to the design, modeling, and fabrication of measurement systems for industrial applications. His research interests include contactless transmissions between sensors and electronics, contactless activation for resonant sensors, and signal processing for microelectromechanical systems.